ROLE OF LIGHT AND HEAVY IONS ON GRAPHENE GROWTH VIA PECVD TECHNIQUE

A Dissertation submitted in partial fulfillment of the requirement for the Award of degree of

MASTER OF TECHNOLOGY

IN

NUCLEAR SCIENCE & ENGINEERING (NSE)

BY

IRFAN AHMAD
(2K15/NSE/03)

Under The Guidance of

Prof. S. C. Sharma
Department of Applied Physics
Delhi Technological University
Delhi

DELHI TECHNOLOGICAL UNIVERSITY

(FORMELY DELHI COLLEGE OF ENGINEERING)

DELHI-110042

JULY 2017

CANDIDATES'S DECLARATION

I do hereby certify that the work presented is the report entitled **"ROLE OF LIGHT AND HEAVY IONS ON GRAPHENE SHEET GROWTH VIA PECVD TECHNIQUE"** in the partial fulfillment of the requirements for the award of the degree of "Master of Technology" in Nuclear Science Engineering submitted in the Department of Applied Physics, Delhi Technological University, is an authentic record of my own work carried out from January 2017 to July 2017 under the supervision **of Prof. S. C. Sharma**, Department of Applied Physics

I have not submitted the matter embodied in the report for the award of any other degree or diploma.

Date: 28/07/2017

IRFAN AHMAD
2K15/NSE/03

CERTIFICATE

This is to certify that above statement made by the candidate is correct to best of my knowledge.

Prof. S. C. Sharma
Department of Applied Physics
Delhi Technological University
Delhi

ACKNOWLEDGEMENT

I take this opportunity as a privilege to thank all individuals without whose support and guidance I could not have completed my project successfully in this stipulated period of time. First and foremost I would like to express my deepest gratitude to my supervisor **Prof. S.C. Sharma**, HOD, Applied Physics, for his invaluable support, guidance, motivation and encouragement throughout the period this work was carried out.

I am also thankful to **Mr. Ravi Gupta** and **Ms. Neha Gupta** (Research scholars) for their valuable support and guidance in carrying out this project.

I am deeply grateful to **Dr. Nitin K. Puri** (Assistant Professor, Applied Physics, Branch Coordinator, NSE) for his support and encouragement in carrying out this project.

I also wish to express my heartful thanks to staff at Department of Applied Physics of Delhi Technological University for their goodwill and support that helped me a lot in successful completion of this project.

.

Irfan Ahmad
2K15/NSE/03

ABSTRACT

A theoretical modelling for the catalyst-assisted growth of graphene sheet in the presence of plasma (Ar + H_2 + C_2H_2) has been investigated. It is observed that the plasma composition can strongly affect the growth and field emission properties of graphene sheet. The effect of plasma compositions (i.e., different concentration of participating ions) on growth, structure and field emission properties Graphene sheet has been theoretically investigated. In plasma, two different kinds of positively charged ions with heavy (Acetylene, $C_2H_2^+$) to light (Hydrogen, H^+) ion, with neutral mass ratio of 13 are considered and the effect of the different fractional concentrations of participating ions on the growth and field emission properties of graphene is studied.

Numerical calculations of the graphene sheet dimensions (height, thickness) for different fractional light ion concentrations have been carried out for the graphene growth via PECVD. It is found that on increasing fractional light ion concentration, the thickness and height of graphene sheet decreases and consequently the field emission factor for graphene sheet increases.

CONTENTS

LIST OF FIGURES

LIST OF TABLES

NOMENCLATURE

n_{po}	=	Plasma density
n_{eo}	=	Electron density
a_l	=	Fractional density of light positive ion
a_h	=	Fractional density of heavy positive ion
n_{ilb}	=	Densities of light ion
n_{iha}	=	Densities of heavy ion
f_{iz}	=	Ionization frequency
v_{kn}	=	Collision frequency with the neutrals
γ_e	=	Sticking coefficient of electrons
n_{CH}	=	Surface concentration of CH
ϑo	=	Number of adsorption sites per unit area
δE_i	=	Thermal energy barrier
ρ_{gn}	=	Graphene sheet density
C_p	=	Specific heat capacity of graphene sheet
ε_{egn}^{s}	=	Mean energy of electrons collected by graphene
ε	=	Emissivity of the material of the graphene sheet
σ	=	Stefan–Boltzmann constant

Chapter 1: Introduction

1.1 Introduction

In 2004 A.D. persistent efforts of scientist A. K. Geim and K. S. Novoselov bore fruits when they isolated the graphene for the first time with a relatively rudimentary technique called micro mechanical cleavage [1].They achieved success with almost a bench top apparatus in which they held a layer of graphite between two faces of folded sticky tapes and when they are unfolded it tears away some layers .Numerous iterations of the above process high crystalline quality of graphene sheets .After this for their further "Pioneering work in Graphene" in explain its exotic properties and explaining its behaviour they were awarded the Noble Prize in Physics in 2010 A.D. Since then a spate of scientific research has begun which is aptly termed as **THE RISE OF GRAPHENE**

Here, in the present work the growth of graphene sheet is done in the presence of plasma through Plasma Enhanced Chemical Vapour Decomposition (PECVD) process. Plasma is considered as it is advantageous over other methods. In plasma the incident particle has high energy due to ionization as compared to neutral atoms in other processes. This increased energy provides high particle reactivity, control of the surface reactivity. Hence the graphene sheet produced by this process have improved structure, crystallinity and ordering [2].

In the present work, a silicon substrate is used in a stainless steel cylindrical plasma reactor. On this substrate, a layer of catalyst is laid. Here the catalyst used is copper. Then a mixture of gases including hydrocarbon, hydrogen and argon is introduced in the chamber. The plasma ionizes the various gases present in the chamber to form mixture of ions, electrons, and neutral atoms. Hence multiple species are present which ionize, combine, and dissociate continually to form new species through various chemical reactions. These active species dissociate the catalyst particle to form nanoparticles on which the accretion of carbon atom takes place and hence the graphene sheet grows.

1.2 Thesis Outline

This thesis aims to provide the general introduction to graphene and its exceptional properties and other related information in addition to the fundamental research work that has been carried out in it. In no way this should be taken as an exhaustive treatment of graphene properties as there are other excellent resources available for that but I firmly believe that this can surely serve as a starting point for anybody and provide a glimpse into the wonderful world of graphene. *Chapter 2* dwells into the theoretical background associated with graphene and how it eventually came onto the big picture electrical, mechanical and optical properties of graphene. It elaborates into the different method of graphene synthesis and pros and cons associated with them. The same chapter deals with the characterization techniques that are used to differentiate the graphene and also its types like single layer, double layer and few layer graphene. It also gives information about the potential applications and recent trends in the industries. In *Chapter 3* provides details about the growth of graphene and Effect of Plasma on growth of graphene. *Chapter 4* deals with the methodology and theory used in the calculations. *Chapter 5* elaborates on the simulation results and discusses the underlying cause and effect. *Chapter 6* draws the conclusion from the results and discussion and also discusses the future scope of the work.

Chapter 2: Graphene

2.1 Brief History of Graphite in relation to Graphene

In other cases the insertion of guest molecules may occur through covalent bonding via chemical grafting reactions within the interlayer space of graphite; this results in structural modifications of the graphene planes because the hybridization of the reacting carbon atoms changes from sp2 to sp3. A characteristic example is the insertion of strong acids and oxidizing reagents that creates oxygen functional groups on the surfaces and at the edges of the graphene layers giving rise to graphite oxide. . Schafheutl [3] first (1840) and Brodie [4] 19 years later (1859) were the pioneers in the production of graphite oxide. The former prepared graphite oxide with a mixture of sulfuric and nitric acid, while the latter treated natural graphite with potassium chlorate and fuming nitric acid. Staudenmaier [5] proposed a variation of the Brodie method where graphite is oxidized by addition of concentrated sulphuric and nitric acid with potassium chlorate. A century later (1958) Hummers and Offeman [6] reported the oxidation of graphite and the production of graphite oxide on immersing natural graphite in a mixture of H2SO4, NaNO3, and KMnO4 as a result of the reaction of the anions intercalated between the graphitic layers with carbon atoms, which breaks the aromatic character. The strong oxidative action of these species leads to the formation of anionic groups on graphitic layers, mostly hydroxylates, carboxylates, and epoxy groups. . The out of planar C–O covalent bonds increase the distance between the graphene layers from 0.35 nm in graphite to about 0.68 nm in graphite oxide [7]. This increased spacing and the anionic or polar character of the oxygen groups formed impart to graphene oxide (GO) a strongly hydrophilic behaviorThus graphite oxide becomes highly dispersible in water. The formation of sp3 carbon atoms during oxidation disrupts the delocalized π system and consequently electrical conductivity in graphite oxide deteriorates reaching between 103 and 107 Ω cm depending on the amount of oxygen [2, 8].In other cases the insertion of guest molecules may occur through covalent bonding via chemical grafting reactions within the interlayer space of graphite; this results in structural modifications of the graphene planes because the hybridization of the reacting carbon atoms changes from sp2 to sp3. A characteristic example is the insertion of strong acids and oxidizing reagents that creates oxygen functional groups on the surfaces and at the edges of the graphene

layers giving rise to graphite oxide. Schafheutl [3] first (1840) and Brodie [4] 19 years later (1859) were the pioneers in the production of graphite oxide.

2.2 Graphene

Graphene is a single layer of carbon packed in a hexagonal (honeycomb) lattice, with a carbon-carbon distance of 0.142 nm. It is the first truly two-dimensional crystalline material and it is representative of a whole class of 2D materials including for example single layers of Boron-Nitride (BN) and Molybdenum-disulphide (MoS2), which have both been produced after 2004. For several decades the isolation of graphene monolayer seemed to be impossible on the basis of, among other things, theoretical studies on the thermodynamic stability of two-dimensional crystals [9]. An important step in this direction was made by a research group in Manchester guided by Geim and Novoselov in 2004 [10] who reported a method for the creation of single layer graphene on a silicon oxide substrate by peeling the graphite by micromechanical cleavage (scotch tape method). Graphene exhibited outstanding structural [11], electrical [12], and mechanical properties [13] and 6 years later Novoselov and Geim were honored with the Nobel Prize in Physics ‘‘for groundbreaking experiments regarding the two-dimensional material graphene.’’ During this time a number of methods for the production of graphene monolayers have been developed. These methods can be divided into different categories depending on the chemical or physical process employed to obtain the single layer graphene.

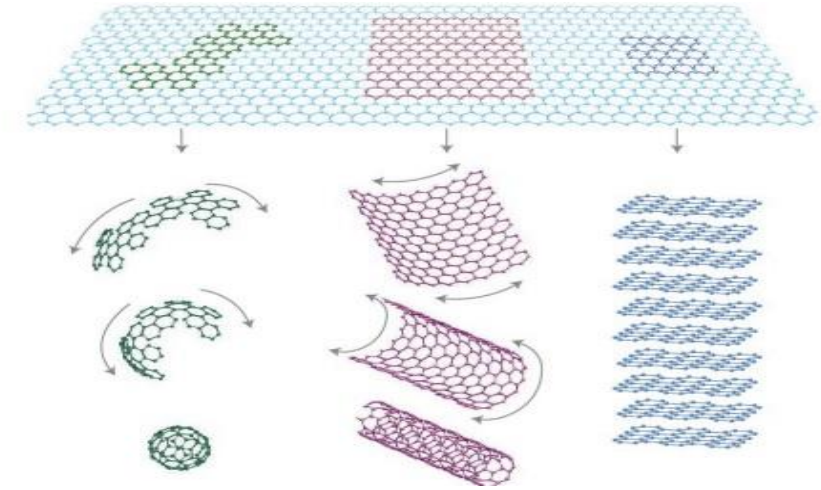

Figure 2.1 C60 fullerene molecules, carbon nanotubes, and graphite can all be thought of as being formed from graphene sheets, i.e. single layers of carbon atoms arranged in a honeycomb lattice,[13]

2.3 Graphene Synthesis

Mass production of graphene of highly crystalline quality and free from defects on an Industrial scale still possesses a formidable challenge among researchers. Until this dream is realized graphene wouldn't be able to replace material in devices used in everyday life thus wasting the trove of exceptional electronic and structural properties it holds. Graphene fabrication can be categorized into two methods namely called top down approach and bottom up approach. In top down method van der wall forces that holds the graphite layers are annihilated to provide us with monolayer and few layer graphene sheets. This is mainly achieved by the micromechanical cleavage of graphite and exfoliation of graphite intercalated compounds (GICs) .While micromechanical cleavage is very labour intensive procedure, exfoliation requires great care in maintaining the sheet quality and preventing the reattachment of flakes. In bottom up methods graphene flakes are grown on substrate from various sources of carbon. Both methodologies have their share of advantages, disadvantages and constraints associated with them. Low production and large number of steps involved in top down practice has restricted its application only to laboratory research, while high temperature is the essential requirement for high quality graphene production in bottom up approach thought they are still inferior in quality as compared to one's produced in top down. Prime concerns in quality mostly pertain to its electron mobility that are affected by method of fabrication used due to a number of defects and type of substrate employed in it.

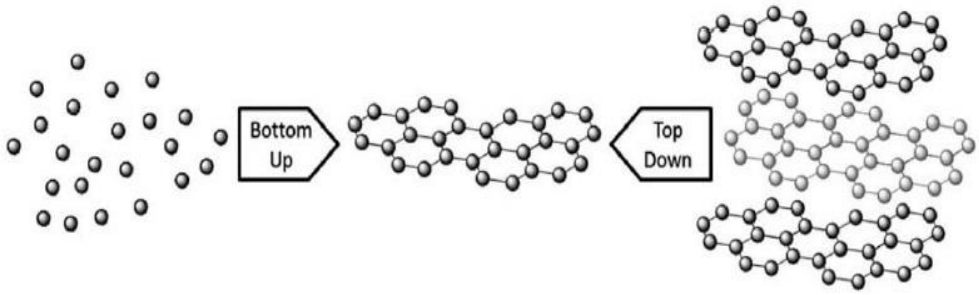

Figure 2.2 Top down and bottom up graphene synthesis scheme [14]

The choice of method also depends on the final technological application as there are varied requirements ranging from transparent electrodes to thin films employed in sensors whereas batteries and super capacitors require large amount of graphene platelets and nanosheets. This shows that while some properties are paramount to certain application, they have no such utility in other application for example thermal conductivity is required in polymer composite but not as such in electrodes. In contrast electron mobility and chemical inertness are very important in every application and it is insured that they remain intact in every fabrication method. Moreover sometime the very nature of method affect the choice too for example silicon carbide (SiC) is used as insulating substrate if it is used in electronics devices that need to be operable at room temperature while if it is grown on a metal that will require an additional step of transferring to insulation substrate. All these considerations fairly affect the choice of method of synthesis.

Top down Approaches

2.3.1 Micromechanical Cleavage.

Using this technique also called "scotch tape method" and "peel off method", K. S. Novoselov and A. K. Geim were the first ones who were able to isolate monolayer and few layer graphene (FLG) from highly oriented pyrolytic graphite (HOPG) which was used as a precursor. Adhesive tape was used to tear apart the layer in successive manner by overcoming the weak van der wall forces that holds the layers together .Flakes were then transferred on SiO2/Si (300 nm oxide layer) substrate and observed under optical microscope. As there was no characterization technique available for graphene at that time and graphene is almost transparent, it was no less than a serendipity that they were found. It was due to change in the refractive index and colour of the silicon oxide substrate and graphene layer when they were deposited on them. Monolayer, bi-layer, tri-layer and few layer graphene of very high quality can be obtained by this technique and easily characterized by this as they all change the colour of the substrate to different one. Synthesis by any other method does yield does not such high quality graphene but still its application is only limited principle research owing to tedious labour it requires an abrupt edges in final product.

2.3.2 Exfoliation Technique

High hopes are pinned on this technique for mass production of graphene though there are still some issues that needed to be tackled. This technique mainly deals with exfoliation of graphene intercalation compounds and graphene oxide .Exfoliation works by inserting foreign molecules between the layers and widening the gap thus weakening the inter layer attractive forces. This helps in breaking the predecessor material into individual graphene layers. One such method is to use sulphuric acid – potassium hydroxide [15] with surfactant [16] and graphite. [SO4]2- ions are responsible for intercalation thus making H2SO4 a good electrolyte whereas surfactant prevent stockpiling of sheets though they can tough to detach later [16] alongside adversely affecting graphene layer's electronic properties. Flakes of different thickness are then separated by centrifugation. Graphite intercalation compounds which are formed by reaction of reducing agents or oxidising agent or salts with graphite followed by sonication in solvents or thermal expansions or gaseous expansions.

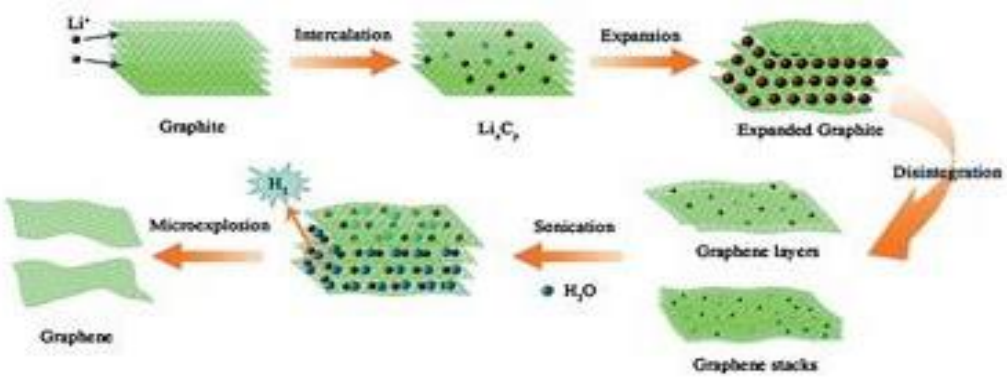

Figure 2.3 Sketch showing formation steps of graphene sheets through Li Intercalation-expansion-micro explosion processes [17]

Bottom up Approaches

2.3.3 Epitaxial Silicon Carbide Growth

Graphene can be synthesized by the thermal decomposition of silicon carbide at very high temperature followed by subsequent rearrangement of carbon atoms to form graphene layers that are left behind after the sublimation of silicon atoms from top of

the surface .Process requires very high temperatures (excess of 1000 ^{o}C) and ultrahigh vacuum conditions though growth in inert gas atmosphere (argon) has been demonstrated too [18]. Different conditions produces different type of graphene with different properties varying in thickness and defects. Argon allows the use of higher temperature (1500 ^{o}C) that benefits in much better quality graphene as it drastically lower the rate of silicon sublimation making carbon atom more mobile. Hexagonal silicon carbide is generally used for graphene fabrication. Both carbon rich and silicon rich surface can be used synthesis and both results in graphene with varying quality levels. Si rich surface requires higher temperature thus giving better quality graphene of usually few layers that exhibits Bernal stacking [19] and that's why it is more studied of two. While carbon surface exhibits rotational stacking [19] requiring low temperatures and giving graphene with more layers (>10).Major challenges in this method includes the stringent requirements of high temperature and vacuum conditions. Though nickel catalysed low temperature growth (700-800 ^{o}C) has been demonstrated but this spikes up the cost of fabrication owing to the costly transition metal nickel [20].This method is most suitable for the wafer based electronics devices as there is no need to transfer graphene on insulating substrate. Moreover it would be interesting to see how this method is used in economically viable devices as SiC is costly material.

2.3.4 Chemical Vapour Deposition

Carbon rich gases are broken down using pyrolysis at very high temperature in this method to grow monolayer and few layer graphene. Chemical vapour deposition can be divided into two routes where in first route the carbon containing gases are decomposed on the metal substrate to form monolayer graphene through surface catalyses and in other routes formation occurs by the segregation of carbon dissolved in metal bulk .the segregation on the top of metal surface upon cooling as solubility of carbon is decreased to a very low level giving multi-layer graphene which can be controlled by the cooling rate and the quantity of carbon dissolved in metal and their alloys namely with growth conditions and graphene quality varying from metal to metal .Nickel and Copper have been extensively used and researched for chemical vapour deposition of graphene .Graphene growth on nickel occurs through the segregation method in which the mixture of methane and hydrogen is decomposed on the nickel bulk and dissolved in it temperature above the 1000 ^{o}C . When the bulk is cooled down the metal precipitates out of the bulk and segregate on the surface of

metal forming few layer graphene. Different rate of bringing down the temperature in this method greatly affects the quality and thickness of graphene in addition to obliterating the requirement of high vacuum conditions .On copper the growth occurs through the decomposition of carbon rich gas on its surface. This is due to the fact the solubility of carbon is very low in copper metal and thus forming a monolayer of graphene on the copper substrate. The interaction between the metal and carbon also need to be taken care as metal has to be scratched off without damaging the graphene layer mostly done by spin coating technique. Other disadvantages in this method include high temperature and vacuum conditions required

2.4 Some properties of graphene

Density of graphene The unit hexagonal cell of graphene contains two carbon atoms and has an area of 0.052 nm2. We can thus calculate its density as being 0.77 mg/m2. A hypothetical hammock measuring 1m2 made from graphene would thus weigh 0.77 mg.[21]

Optical transparency of graphene Graphene is almost transparent, it absorbs only 2.3% of the light intensity, independent of the wavelength in the optical domain. This number is given by $\pi\ \alpha$, where α is the fine structure constant. Thus suspended graphene does not have any colour.[21]

Strength of graphene Graphene has a breaking strength of 42N/m. Steel has a breaking strength in the range of 250-1200 MPa= 0.25-1.2x109 N/m2. For a hypothetical steel film of the same thickness as graphene (which can be taken to be 3.35Å=3.35x10-10 m, i.e. the layer thickness in graphite), this would give a 2D breaking strength of 0.084-0.40 N/m. Thus graphene is more than 100 times stronger than the strongest steel. In our 1 m2 hammock tied between two trees you could place a weight of approximately 4 kg before it would break. It should thus be possible to make an almost invisible hammock out of graphene that could hold a cat without breaking. The hammock would weigh less than one mg, corresponding to the weight of one of the cat's whiskers.[21]

Electrical conductivity of graphene The sheet conductivity of a 2D material is given by σ = enμ. The mobility is theoretically limited to μ=200,000 cm2V−1s−1 by acoustic phonons at a carrier density of n=1012 cm−2. The 2D sheet resistivity, also called the resistance per square, is then 31 Ω. Our fictional hammock measuring 1m2 would thus have a resistance of 31 Ω. Using the layer thickness we get a bulk conductivity of 0.96x106 Ω-1cm-1 for graphene. This is somewhat higher than the conductivity of copper which is 0.60x106 Ω-1cm-1.[21]

Thermal conductivity The thermal conductivity of graphene is dominated by phonons and has been measured to be approximately 5000 Wm−1K−1. Copper at room temperature has a thermal conductivity of 401 $Wm^{-1}K^{-1}$. Thus graphene conducts heat 10 times better than copper.[21]

2.5 Graphene Applications

2.5.1 Medicine

Graphene is being investigated as a reinforcing agent in tissue engineering applications considering its tensile strength and other highly rated mechanical properties .When grapheme in powdered form is mixed in polymer matrix, cross-linking density is improved in nanocomposite thus imparting them better load handling capability. It has also being tried as a contrasting agent for magnetic resonance imaging and thermo acoustic tomography .it has also been reported that due to its thermal conductivity it can also catalysed polymerase chain reaction through the increase of DNA product yield. Graphene has a large surface area and can be easily be modified and bent thus finding application in bio sensors and diagnosis devices. It has been also found the low level concentration of graphene nanoribbons are nontoxic in nature and does not harm the stem cells ,therefore can be used for drug delivery system in cancer treatment to kill cancerous cells.

2.5.2 Electronics

Most of the future of graphene is seen in the field of electronic devices given its high carrier mobility and associated low noise. Graphene has ability to replace silicon in electronics devices with much faster speed and smaller size if its limitations are removed. Gated graphene has low on/off ratio of order around 10 depending on graphene's quality and gating effectiveness, while to make digital switch the ratio required in digital transistor is 104.This can be attributed to its zero band gap property. This is biggest hurdle in its way to become an effective logic gate. A lot of research has been done in this field to open a band gap including quantum confinement in graphene by cutting into nanoribbons but no major breakthrough has been achieved in this field. IBM has already designed and fabricated graphene based transistor and integrated circuit which is a broadband mixer that can work up to of frequencies of 10 GHz and temperature of 127 ^{o}C though it suffer from low voltage gain. Graphene also have a great potential to substitute for indium tin oxide as a transparent conducting film in solar devices, light emitting diodes and other displays. Given ITO has available in limited quantity and due to its rising cost the need for replacement is greater than ever. Merits of graphene in this case include higher optical transparency (98%) than ITO (90%) and mechanical flexibility whereas ITO is brittle. That's why graphene can find great application in wearable electronics. Only hurdle in this application is its very high electrical resistance offered by graphene sheets than ITO. Some progress in this direction to reduce resistance has been made by increasing the number of layers and treating with nitric acid both at the cost of reduced transparency. Hall effects sensors with very high sensitivity have been developed from graphene that may find applications with DC current transformers. Graphene fabricated using chemical vapour deposition technique on SiO_2 substrate has been found to preserve their spin for a long time and this can be used in spintronics application where spin is used a data at the place on current state. This can be used in data storage disks and magnetic random access memory. It shows sensitivity to infrared spectrum at room temperature and thus can also be effectively used in infrared devices and contact lenses.

2.5.3 Energy

Membranes of graphene oxide are impermeable to gases and liquid but allow water vapour to pass through it. This property has been used to effectively distil alcohol to higher concentration at room temperature with traditional vacuum distillation method and can be further utilized into better biofuel economies. Graphene's high optical transparency and electron mobility find great application in solar devices with better conversion efficiency than silicon based devices. It is also found that graphene let protons pass through it thus raising the hopes for better and efficient fuel cells. Considering graphene large surface area one potential application is in super capacitors' conductive plates .Graphene based micro super capacitors have been demonstrated.

Chapter 3: Growth of Graphene and Effect of Plasma on Growth of Graphene

3.1 Review of Previous Work

Much research has already occurred into the characteristics of CVD graphene growth, as well as the possible improvements PCVD can offer. For CVD, multiple groups have already determined that Cu substrates at very low pressures can grow single layer graphene without producing additional layers during growth.[22] Similarly, it is believed that polycrystalline metallic substrates work best for growing graphene epitaxially, as the domain size for planar grapheme grown on polycrystalline metals matches for both of them.[22] This trend suggests that for crystalline carbon formations to form polycrystalline substrates are required to help structure the growth.

When it comes to incorporating plasma into the CVD system, there are two general methods. One places the plasma-generating electric field around the substrate, which encases it in a shell of plasma. This method has been shown to affect the growth of graphene, causing the graphene film to grow in the direction of the electric field and thus perpendicular to the substrates surface. This is similar to how carbon nanotubes are grown, and yields grapheme flakes.[22]

The other method for incorporating plasma is to add a remote source, which our experiment has done. A remote source will not affect the direction of the carbon crystal's formation and thus allows for planar growth of graphene films.[22] This allows for the possibility of multiple layers of growth, as well as larger graphene sheets for the production of nanoelectronic materials.

Also with a remote rf plasma source, the flow of hydrogen has been shown to produce more pronounced peaks in the Raman signals. This results from a relatively high concentration of atomic hydrogen from inductively coupled plasma, which helps to etch amorphous carbon from the substrate at a high rate than sp2 hybridized carbon.[22] Thus, by flowing hydrogen during growth, it helps to promote the growth of higher quality graphene over the growth of amorphous carbon.

3.2 Brief Introduction to PECVD

The experimental setup for PECVD consists of three main parts including the gas, the plasma generator and the vacuum heating chamber, as illustrated in **Figure 3.1**. Other setups where the plasma generators and the growth chamber are combined are also widely used in PECVD growth. Plasma generator is the core of the PECVD, can mainly be categorized into three types depending on the power source for plasma generation, i.e., microwave (MW) plasma (commonly 2.45 GHz), radio frequency (RF) plasma (commonly 13.56 MHz) and direct current (dc) plasma. The MW plasma is a type of high-frequency electromagnetic radiation in the GHz range. To date, MW-PECVD has been used extensively in the synthesis of graphene and its derivatives such as CNTs, nanowalls and diamond films. RF plasma is another popular source with domain frequency in MHz range. The energy of an RF generator is coupled to the plasma in three main modes: the evanescent electromagnetic (H) mode, the propagating wave (W) mode and the electrostatic (E) mode W-mode. H-mode inductively coupled plasma (ICP) has the advantage of high energy density and a larger plasma volume, thus yielding high growth rates. In contrast, E-mode capacitively coupled plasma cannot be used as an independent plasma source due to relatively low energy. As the simple setup, dc glow plasma is also widely used source. There are two geometric designs for dc glow plasmas: parallel-plate and pin-to-plate, which can produce uniform and nonuniform plasma sources, respectively.

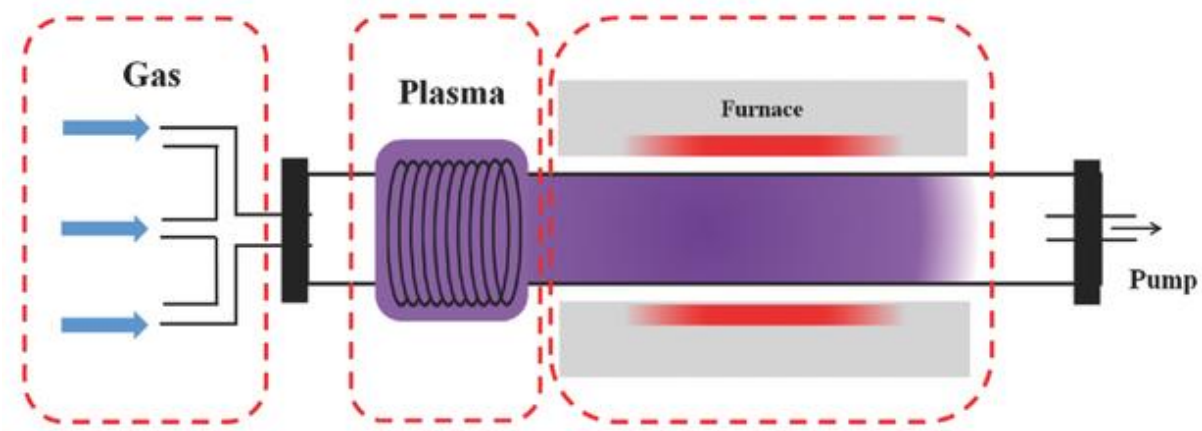

Figure 3.1 Schematic of experimental setup for PECVD including gaseous system, plasma generator system, and vacuum heating system.[39]

Gaseous species are essential for the synthesis of graphene and its derivatives, which can be categorized into three functional groups. (i) The gaseous precursors containing carbon provides carbon radicals for graphene growth via plasma-enhanced reaction. (ii) Gases such as H_2, O_2 are added as amorphous carbon etchants to produce high-quality graphene and its derivatives. (iii) Gases such N_2, NH_3 normally are used to achieve the doping of as-grown graphene, which can tailor the electrical properties of graphene.

During the plasma-enhanced process, the source gas is activated by the energetic electrons generated in the plasma. The ionization, excitation, and dissociation of the source gases all occur in the low-temperature plasma process. First, the ionization processes proceed via interactions between energetic electrons and gas molecules. Second, high-energy ions generated in ionization processes subsequently react with source gas molecules. Finally, various radicals form via various dissociation reactions. These radicals are more reactive than ground-state atoms or molecules, which enable the formation of graphene and its derivatives on catalyzed or noncatalyzed surfaces at low temperature. In order to optimize the synthesis process, the plasma-enhanced process needs to be understood theoretically and experimentally.

Simulations of the plasma process have been performed to optimize the growth parameters. A number of plasma models have been developed based on different gas systems.[23-25] In these models, tens of species (ions, electrons, neutrals and radicals) and reactions are considered. For the methane or methane/hydrogen plasma, 8 neutrals, 11 ions and 5 radicals have been taken into account in 1D fluid model.[26] 27 electron reactions, 7 ion-neutral reactions and 12 neutral-neutral reactions are included in this model. The densities of radicals and ions are found to vary with distance in the plasma based on 1D fluid models. Extending to the radial directions, 2D fluid model is proposed.[27]

Besides the CH_4 and CH_4/H_2 systems, several models are also used for the $Ar/CH_4/H_2$,[28] $Ar/C_2H_2/H_2$,[29] $Ar/C_2H_2/NH_3$,[30] CH_4/NH_3, and C_2H_2/NH_3 systems. For gas systems including Ar, Ar atoms become the dominant neutrals in all species.[27,28] The densities of CH_4 and H_2 decrease more dramatically with the plasma power. For nonradical and radical neutrals, higher hydrocarbons (C_xH_y) are more likely to break into radical fragments due to more intense electron-neutral reactions in Ar plasma, compared to the CH_4 and CH_4/H_2 systems. In the plasma

models containing NH_3, additional 22 species, 43 electron-impact reactions, 48 ion-neutral reactions and 67 neutral-neutral reactions should be considered. For the $Ar/C_2H_2/NH_3$ systems,[30] atomic hydrogen can be produced from C_2H_2 and NH_3 dissociation reactions.

Plasma-enhanced process is a complicated process containing various kinds of species and reactions, which play an important roles in the plasma-enhanced growth process of graphene. For example, the density of carbon related species can influence the morphology of the as-grown graphene. Additional species such as H_2, Ar can serve as amorphous carbon etchant toward high-quality graphene. Other additional species such as NH_3, N_2 can dope graphene with heteroatoms and adjusting the electrical properties. All simulative and experimental results above offer information about these species and reactions, which contribute to understanding kinetic growth in the plasma process, which are of great significance to realization of the controllable synthesis of graphene.

3.3 Mechanism of Graphene Growth by PECVD

3.3.1 Nucleation and Coalescence Mechanism

In thermal CVD process, the graphene can be grown on the surface of the transition metals by surface catalytic decomposition mechanisms. The metal catalyzed growth of graphene involves surface processes including dissociation of hydrocarbon molecules, formation of C clusters, surface diffusion and extension of graphene nuclei.[34] It is believed that the attachment of C clusters generated by surface catalytic decomposition to graphene nuclei is very important for the growth of high-quality graphene films in metal catalyzed CVD. However, the nucleation process is largely enhanced due to more reactive radicals generated in plasma-enhanced dissociation reactions. The nucleation and coalescence would be more important for plasma-enhanced growth of the graphene, especially at low temperature or without metal catalysts.

Koichiro Saiki et al. have reported the growth of graphene by PECVD on catalytic metal surfaces, and related mechanisms are also discussed in detail.[31]It has been widely reported that Cu surface has a catalytic effect that dissociates hydrocarbons into the activated carbon species. However, the catalyzed dissociation process cannot occur at the temperature below 600 °C. At low growth temperature, only activated

carbon radicals generated by the plasma contribute to growth process of graphene on Cu surface. The graphene growth process is dominated by nucleation and coalescence of graphene patches with size of ≈20 nm, as shown in **Figure 3.2**a.

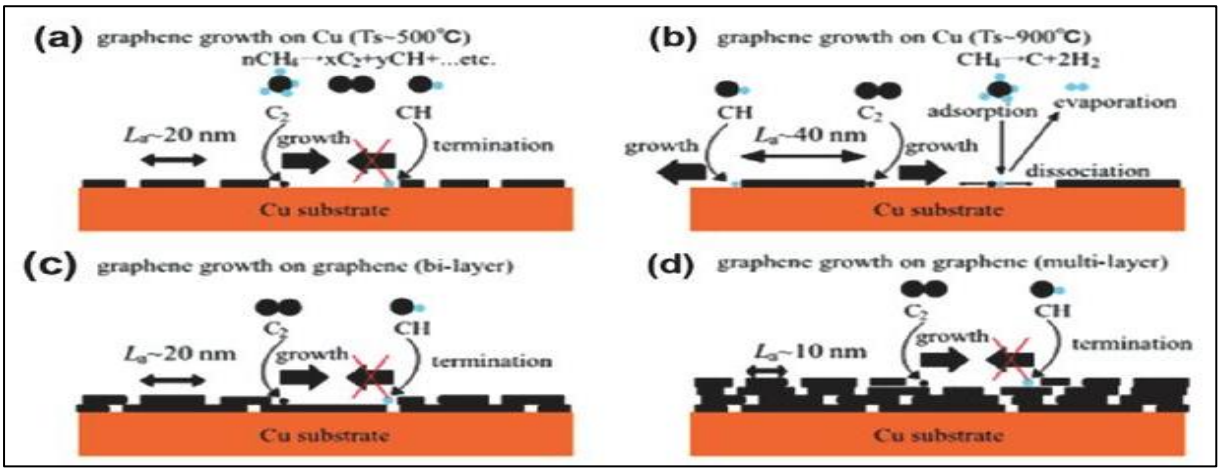

Figure 3.2 Schematic of growth mechanism on Cu substrate by PECVD. a) Monolayer growth at low growth temperature (500 °C). b) Monolayer growth with larger grain size at high growth temperature (900 °C). c) Secondary layer growth on the first layer. d) Successive layers growth. [31]

Increasing the growth temperature to 900 °C, the catalytic effect of Cu arises. In the graphene growth process, carbon radicals can be generated by plasma-enhanced and metal-catalyzed dissociation. The activated carbon radicals generated by catalytic dissociation can enlarge the size of nucleated graphene patches to ≈40 nm, as shown in **Figure 3.2b**. After the growth of the first layer graphene on Cu, activated carbon radicals cannot be generated by metal catalyzed dissociation. Small graphene patches rather than enlarged graphene domains nucleate and coalesce into the second layer graphene, as shown in **Figure 3.2c,d**. Successive layer graphene can also be grown by the mechanism of nucleation and coalescence with smaller crystal size ≈10 nm. The growth of the graphene on noncatalyzed substrates can be fully dominated by nucleation and coalescence mechanism. As reported by Zhang et al. catalyst-free growth nanographene films can be achieved on noncatalyzed SiO_2/Si, Al_2O_3, mica, silica and even glass with low growth temperature.[32,33] Nanographene islands with different sizes and heights first form in the growth process. With longer growth duration, more nanographene islands nucleate and coalesce into continuous films.

3.3.2 Etching and Growth Mechanism

In the nucleation and coalescence mechanism, nanographene with domain sizes varying from few to tens of nanometers nucleate on the substrates. The nanographene should be enlarged by edge growth rather nucleation in order to obtain high-quality graphene films. Liu et al. present the competition of etching and growth mechanism in the catalyst-free growth of the graphene by PECVD.[35] In the mechanism, etching and growth processes are found to be dependent on the growth temperature with

inverse trend. According to the mechanism, a two-step strategy is proposed, in which nucleation and edge growth occur in two isolated stages, as shown in **Figure 3.3**. Nucleation at lower temperature followed by edge growth results into larger graphene domains that nucleation at higher temperature. It is expected that continuous polycrystalline graphene film with larger size graphene domain could be obtained via edge growth after low density nucleation process.

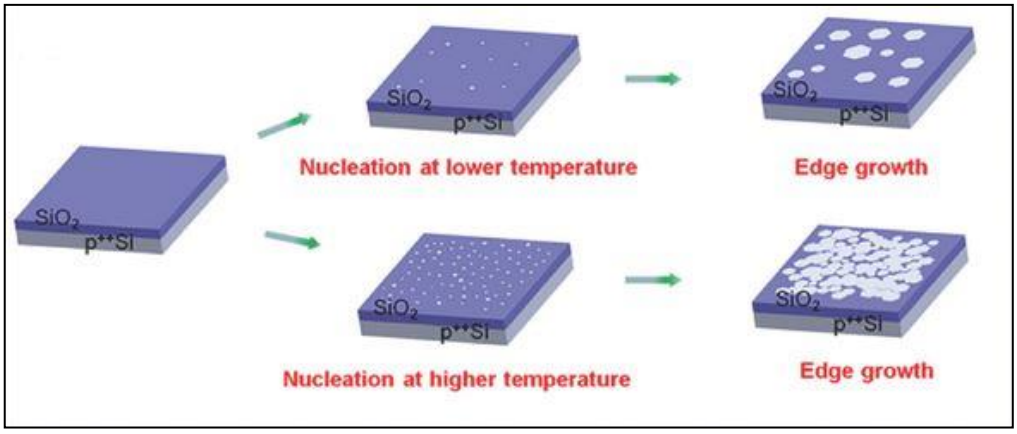

Figure 3.3 Different two-step growth strategies for nanographene growth including isolated stages: nucleation and edge growth.[35]

3.3.3 Vertical Growth Mechanism

Wu et al. first report the successful synthesis of CNWs on sapphire substrate.[36] It is believed that the change of direction of electric field contributes to the formation of CNWs rather than CNTs. It is also reported that horizontally aligned CNTs can be grown on modified SiO_2/Si, which can direct the electric field from plasma to the substrate surface.[37] Therefore, the direction of electric field is essential for the growth of VG nanosheets. However, the growth mechanism of VG nanosheet remains unambiguous. Jiang et al.[38] report that wafer-sized and uniform vertically standing graphene (VSG) films on Cu foil can be grown by using MP-CVD system.[38] **Figure 3.4** shows the mechanism of the growth of the VSG films. First, the hydrocarbon is decomposed and absorb on the surface of the Cu, leading to the growth of 2D multilayer graphene films. Then the layer growth turns into vertical growth due to strain and defects accumulated in the as-deposited films. Moreover, plasma can ensure the 3D growth of vertical graphene nanosheets, because reactive carbon radicals generated in plasma would reach the edge frequently and thus diffuse outward. Although the VG nanosheets have been widely grown by PECVD on various

substrates, the vertical growth mechanism of VG nanosheets needs further investigations. The electric field should be considered for the growth direction and the transition from 2D growth to vertical growth should be investigated in detail.

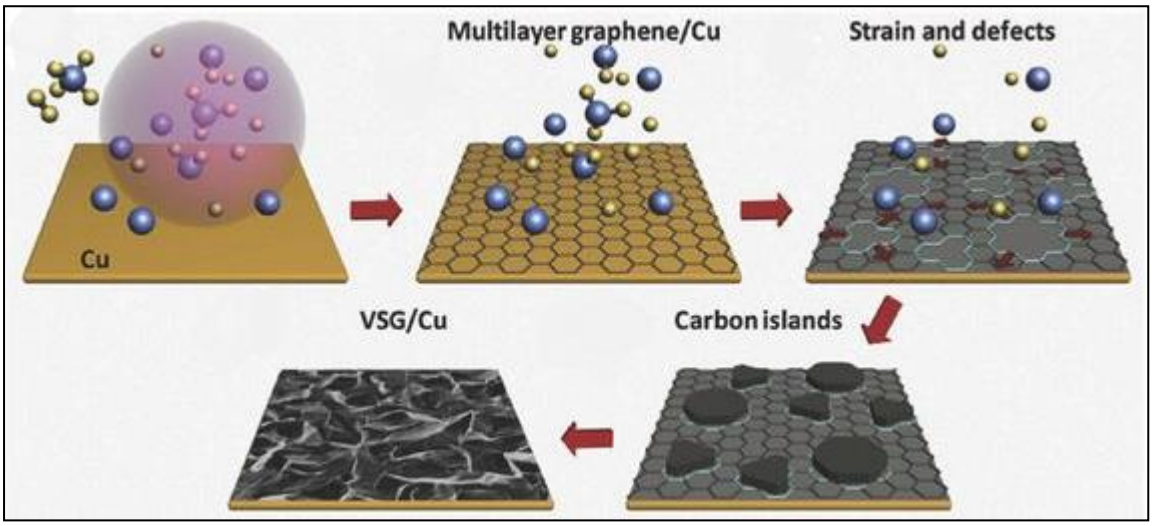

Figure 3.4 Schematic illustration of the growth process of VSG films on copper foil in an PECVD system.[38]

CHAPTER 4: Theoretical Model of Growth of GRAPHENE

In this model, we study the growth of the graphene sheet on the catalyst– substrate surface in the presence of reactive plasma containing electrons, positively charged ions of acetylene ($C_2H_2^+$) represented as ions A and hydrogen ions (H^+) represented as ions B, neutral atoms of type A acetylene (C_2H_2), and neutral atoms of type B hydrogen (H_2). We are taking Silicon (Si) as substrate and Copper (Cu) as the catalyst. The reactive plasma of Ar + H_2 + C_2H_2 is taken and C_2H_2 acts as a main source of carbon.

We consider plasma containing two types of positively charged ions of type A and type B, the two ions have considerable differences in their masses such that we consider ion A to be a heavy and ion B to be light ion.

We have formulated a model where we could find relation in heavy and light ion concentration changing one will eventually results in changing other one.

Considering the densities of light and heavy positive ions $\mathbf{n_{ilb}}$ and $\mathbf{n_{iha}}$ with masses $\mathbf{m_{ilb}}$ and $\mathbf{m_{iha}}$, respectively.

$\mathbf{n_{po}}$,Plasma density = $\mathbf{n_{eo}}$,Electron density,

$\mathbf{a_l}$ = Fractional density of light positive ion,

$\mathbf{a_h}$ = Fractional density of heavy positive ion,&

$a_l + a_h = 1$

So, $n_{ilb} = a_l\, n_{po} = a_l\, n_{eo}$

$n_{iha} = a_h\, n_{po} = (1-a_l)\, n_{eo}$

To further explain graphene growth model in consideration of effect of plasma composition (i.e different concentration of participating ions) , the equations considered are:

a) Sheath equations,
b) Charging of the graphene,
c) Kinetic equation for electron density,

d) Kinetic equations for the positively charged ions density,

e) Kinetic equation for neutral atoms,

f) Kinetic equations for the growth of graphene nuclei,

g) Growth rate equation for the graphene sheet,

h) Energy balance equation for the graphene sheet, &

i) Field enhancement factor.

4.1 Sheath Equations

The sheath kinetics [40] to investigate the structure of sheath formed near the substrate are given below and the electric field within the sheath is assumed to be along z-axis.

$$\left(\hat{\imath}\frac{\partial}{\partial x}+\hat{\jmath}\frac{\partial}{\partial y}+\hat{k}\frac{\partial}{\partial z}\right).\left(n_p\vec{v}_p\right)=\ f_{iz}n_e \qquad \ldots (4.1)$$

$$M_p n_p v_p \frac{dv_p}{dz} = e n_p E - M_p n_p f_{pn} v_p \qquad \ldots (4.2)$$

$$\frac{d^2\varphi(x)}{dz^2} = -4\pi \sum q_p \varepsilon_p n_p \qquad \ldots (4.3)$$

where p refers to either

(i) Electrons (e); or

(ii) $C_2H_2^+$ or H^+ ions

The description of various symbols is given below:

M_p = mass of particle p in plasma,

n_p = number densities of the species p,

v_p = fluid velocity of the particle p,

(x) = sheath potential,

f_{iz} = ionization frequency,

f_{pn} = collision frequency with the neutrals,

q_p = charge of the species p,

ε_p = p-th ion to electron number density ratio,

$\Sigma_p\ \varepsilon_p = 1$, and $0 < \varepsilon_p < 1$ because the electron density is higher in plasma bulk than in the sheath.

4.2 Charging of the graphene

The charge developed on the graphene surface is determined by the accretion of electrons and positively charged ions on the surface of the graphene sheet

$$q'[\tau] = I_{i1gn} + I_{i2gn} - \gamma_e I_{egn} \quad \ldots (4.4)$$

where,

$q\ [\tau]$ is the charge over the graphene sheet,

γ_e is the sticking coefficient of electrons,

I_{ijgn} is the ions collection current of j[th] ion,

I_{egn} is the electron collection current on the graphene surface

The first and second term on the right hand side of Eq. (4.4)describe the charge developed on the graphene surface due to accretion of positively charged ions of type 1 and 2, i.e., ions of acetylene and hydrogen, respectively. The third term represents the decrease in charge due to accretion of electrons at the surface of the graphene sheet.

4.3 Kinetic equation of electron density

$$n'_e(\tau) = (\beta_1 n_1 + \beta_2 n_2) - (\alpha_1 n_e(1 - a_l)n_e + \alpha_2 n_e a_l n_e) - \gamma_e n_e I_{egn} \quad \ldots (4.5)$$

where,

β_1 and β_2 are the coefficient of ionization of the constituent neutral atoms due to external field,

n_e is the electron number density, &

n_1 and n_2 are the number density of neutral types 1 and 2, respectively

Equation (4.5) shows the growth of electron density in the plasma system due to ionization of neutral atoms, recombination of electrons and ions, and electron collection current at the surface of the graphene. The first term on the right hand side of Eq. (4.5) is the gain in electron density per unit time because of ionization of neutral atoms. The second and third terms display the decaying rate of the electron density due to the electron–ion recombination and the electron collection current at the surface of the graphene, respectively.

4.4 Kinetic equation of positively charged ion density

$$n'_{i1}(\tau) = \beta_1 n_1 - \alpha_1 n_e(1 - a_l)n_e - n_{gn} I_{i1gn} - J_{ai1} + J_{desorp1} \quad \ldots (4.6)$$

$$n'_{i2}(\tau) = \beta_2 n_2 - \alpha_2 n_e a_l n_e - n_{gn} I_{i2gn} - J_{ai2} + J_{desorp2} + J_{th} \quad \ldots (4.7)$$

where,

J_{ai1} is the adsorption flux onto the catalyst substrate surface,

$J_{desorpj}$ is the desorption flux from the catalyst–substrate surface, j refers to either 1 or 2 type of ions,&

J_{th} is the flux of type 2 ion (namely, hydrogen) on account of thermal dehydrogenation.

Eqs. (4.6) and (4.7) refer to the growth rate of positively charged ions in plasma system. The first term on the right hand side describes the gain in ion density per unit time on account of ionization of neutral atoms. The next two terms represent the rate of decrease in positively charged ion density due to electron-ion recombination and ion collection current at the surface of the graphene, respectively. The fourth and fifth term denotes adsorption and desorption of ions to/from the catalyst-substrate surface, respectively. The last term in Eq. (4.7) represents the increase in hydrogen ion number density in plasma because of thermal dehydrogenation.

4.5 Kinetic equation of neutral atoms

$$n'_1(\tau) = \alpha_1 n_e(1 - a_l)n_e - \beta_1 n_1 + n_{gn}(1 - \gamma_{i1}) I_{i1gn} - n_{gn}\gamma_1 I_{1gn} \quad \ldots (4.8)$$

$$n'_2(\tau) = \alpha_2 n_e n_e a_l - \beta_2 n_2 + n_{gn}(1 - \gamma_{i2}) I_{i2gn} - n_{gn}\gamma_2 I_{2gn} \quad \ldots (4.9)$$

where,

I_{jgn} is the neutral collection current at the surface of graphene, j refers to either 1 or 2 type of neutral atom,

n_j is the neutral atom density,

γ_j is the sticking coefficient of neutral atom, and

γ_{ij} is the ion sticking coefficient.

Eqs. (4.8) and (4.9) describe the growth rate of number density of neutral atoms of types 1 and 2; the first term of the right side denotes the gain in neutral atom density

per unit time due to electron–ion recombination. The remaining terms represent the decaying rate of neutral atom density due to ionization, gain in neutral density due to neutralization of ions collected at the surface of the graphene, and accretion of neutral atoms of species 1 and 2 on the surface of the graphene, respectively.

4.6 Kinetic equation for the growth of graphene nuclei

Following Sharma and Gupta.[41]

$$\frac{d}{d\tau}\left(\pi R_g^2\right) = \left[\left\{2n_{CH}\vartheta \exp\left(\frac{-\delta E_i}{k_B T_s}\right) + 2\theta_{CH} J_{i1} y_d + 2J_{i1} + \frac{J_{i1}\sigma_{ads} J_{i2}}{\vartheta} + J_c\right\} m_c + \left\{J_{i1}\left(1 - \theta_t\right) + \frac{J_{i1}\sigma_{ads} J_H}{\vartheta} + J_{i1}\exp\left(\frac{-\delta E_i}{k_B T_s}\right)\right\} m_{i1}\right] \times \frac{2\pi R_{cat}}{\pi R_{cat}^2 \rho_{cat}}\left(D_1 \exp\left(\frac{-E_{sdC}}{k_B T_s}\right) + D_2 \exp\left(\frac{-E_{sdCl}}{k_B T_s}\right)\right) \times \left(\frac{1}{I_{i1g}}\right) + \gamma_{C_2H_2}\pi R_{cat}^2 I_{C_2H_2 g} \quad \ldots (4.10)$$

where,

R_g is the radius of the graphene nuclei,

R_{cat} is the radius of the catalyst nanoparticle,

ρ_{cat} is the mass density of the catalyst particle,

$\gamma_{C_2H_2}$ is the neutral atom sticking coefficient, and

$n_{CH}(= \vartheta o \theta_{CH})$ is the surface concentration of CH; [43]

θ_{CH} is the surface coverage by C_2H_2 radicals,[43] .

ϑo (approx 1.3 x 10^{15})is the number of adsorption sites per unit area,[43]

m_c (= 12 a.m.u) is the mass of the carbon atom,

m_{i1} (=26 a.m.u.) is the mass of type 1 (i.e., C_2H_2) ions,

δE_i is the thermal energy barrier (1:87 eV), &

$\left(D_1 \exp\left(\frac{-E_{sdC}}{k_B T_s}\right) \text{ and } D_2 \exp\left(\frac{-E_{sdCl}}{k_B T_s}\right)\right)$ are the surface diffusion coefficients of carbon monomers and C-atom clusters, respectively, with the corresponding activation energies, E_{sdC}= 0:1 eV and E_{sdCl} =0:82 eV, respectively.[42]

In Eq. (4.10), the first term in the first bracket on the right side [43] accounts for the carbon yield on the catalyst surface due to thermal dissociation of acetylene ions (with activation energy of thermal dissociation, δE_i); the second term [43] denotes the

carbon yield due to ion induced dissociation of C_2H_2/ion-induced incorporation of neutrals ; the third term refers the decomposition of acetylene ions, i.e., C_2H_2; the fourth term [43] describes the interaction of ions with atomic hydrogen from the plasma; and the fifth term [43] is the rate of the incoming flux of carbon atoms onto the catalyst particle. The terms in the second bracket refers to the adsorption flux of type 1 ions to the catalyst surface, interaction of adsorbed type 1 ions with atomic hydrogen from plasma, and thermal dissociation of hydrocarbon source gas C_2H_2, respectively. The last term denotes the sticking of neutral atoms of type 1, i.e., acetylene to the Graphene Island.

4.7 Growth rate equation for the graphene sheet

Under the influence of the electric field due to plasma, carbon atoms diffuse at the graphene island boundaries raising the height and thickness of the graphene sheet in the upward direction. The etching of carbon due to hydrogen results in the decrease in the thickness of the graphene.

The scheme of the graphene sheet[41] considered in the model is shown in Fig. 4.1

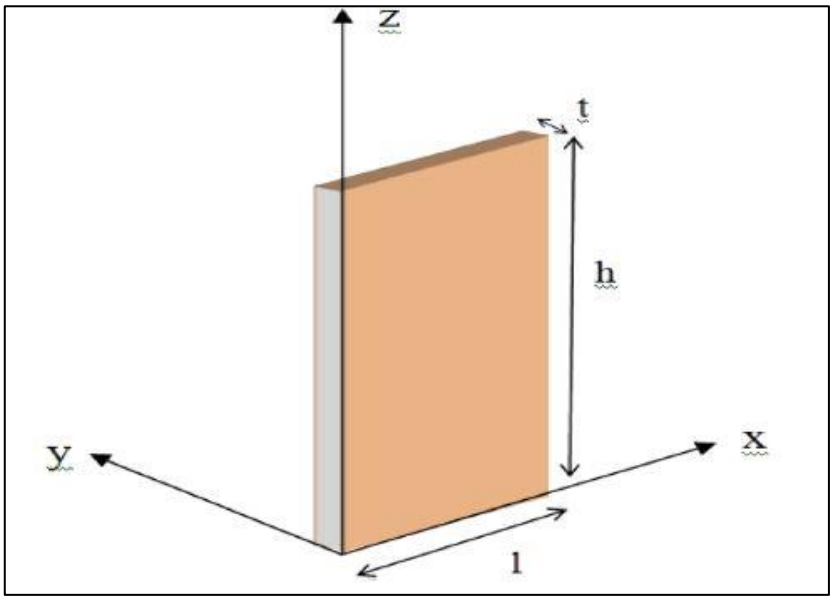

Figure. 4.1. The 3-D view of rectangular graphene sheet.[41]

$$l\frac{d(h\times t)}{d\tau} = \left(\frac{n_1}{\vartheta}\times D_1\, exp\left(-\left\{\frac{E_d+E_{inc}}{k_B T_s}\right\}\right)\frac{\pi R_g^2}{2\pi R_g}\times\left(I_{i1gn}\right)+\left(\gamma_{C_2H_2} I_{C_2H_2gn}\right)\right)\times\frac{M_{gn}}{\rho_{gn}} \quad \ldots (4.11)$$

$$[h(\tau) + l]\frac{d(t)}{d\tau} = \left\{J_{i2}exp\left(\frac{-\delta E_{sdh}}{k_B T_s}\right) + J_{i2}\,(1 - \theta_t) + J_{i2} + \theta_{CH}\left(J_{i2}y_d + \vartheta_0\vartheta\,\exp\left(\frac{-\delta E_i}{k_B T_s}\right)\right)\right\} \times \frac{h(\tau)}{n_e a_l} + \gamma_{C_2H_2}\pi R_{gn}^2 I_{C_2H_2gn} \quad \ldots (4.12)$$

where,

ρ_{gn} is the graphene sheet density and

M_{gn} is the mass of the growing graphene sheet (M_{gn} approx 12 g).

Eq. (4.11) describes the increase in area of the graphene sheet due to diffusion of carbon atoms at the graphene island boundaries, and ion and neutral collection current at the growing graphene sheet. The first term on the right side of the Eq. (4.11) describes the diffusion (with energy barrier, E_d approx 0:13 eV)[44] and attachment of carbon atoms (with energy barrier, E_{inc} approx 0:4 eV)[44] to the border of the growing graphene sheet. The factor I_{i1gn} corresponds to the ion collection on the growing graphene sheet, and the last term accounts the sticking of neutral atoms of acetylene on the graphene sheet.

Eq. (4.12) describes the decrease in thickness of graphene sheet due to etching of carbon by hydrogen atoms. In Eq. (4.12), the first term on the right hand side refers the incoming flux of type 2 ion, i.e., hydrogen due to thermal dehydrogenation of type 1 ions [43]; the second term accounts the adsorption of type 2 ions to the surface. The third term [43] is the decomposition of positively charged ions of type 2; the fourth term [43] describes ion induced dissociation of acetylene; and the fifth term [43] is due to the incorporation of hydrogen ions due to thermal dissociation of acetylene ions. The last term denotes the sticking of neutrals of acetylene on the surface of the graphene sheet.

4.8 Energy balance equation for the graphene sheet

$$RF\ power = \frac{d}{d\tau}\left(M_{gn}C_pT_s\right) = I_{egn}\left[\gamma_e\varepsilon_{egn}^s + (1 - \gamma_e)\delta_{egn}\left[\varepsilon_{egn}^s - \left(\frac{3}{2}k_B\right)T_s\right]\right] - \left(\frac{3}{2}k_B\right)\left[I_{1gn}\left[\gamma_1 T_n + \delta_{1gn}(1 - \gamma_1)(T_n - T_s)\right] + I_{2gn}\delta_{2gn}(T_n - T_s)\right] + \left[I_{i1gn}\left(\varepsilon_{i1gn}^s + I_{z1}\right) + I_{i2gn}\left(\varepsilon_{i2gn}^s + I_{z2}\right)\right] - \left(\frac{3}{2}k_B\right) \times \left[(1 - \gamma_{1i})\,I_{i1gn} +$$

$$I_{i2gn}\,]\,T_s - A\left[\varepsilon\sigma(T_s^4 - T_a^4) + \left[n_1\left(\frac{8k_BT_n}{\pi m_1}\right)^{\frac{1}{2}} + n_2\left(\frac{8k_BT_n}{\pi m_2}\right)^{\frac{1}{2}}\right]k_B(T_s - T_n)\right] \quad \ldots \quad (4.13)$$

where,

$M_{gn}(=(l\times h\times t)\rho_{gn})$ is the mass of the graphene sheet,

$A(=lt+lh+th)$ is the surface area of the graphene sheet,

C_p is the specific heat capacity of graphene sheet (C_p approx 2.1 J g^{-1} K^{-1}),

ε_{egn}^{s} is the mean energy of electrons collected by graphene, [45]

δ_{egn} is the fraction of excess energy of electron lost in a collision with graphene sheet, [45]

δ_{1gn} is the fraction of excess energy of an atom lost in a collision with the graphene sheet,[45]

T_a is the ambient temperature

T_n is the temperature of the neutral atomic species,

I_{z1}&I_{z2} are the ionization energies of neutral atoms 1 and 2, respectively (I_{z1} = 11:26 eV and I_{z2}= 13:5 eV)

ε_{i1gn}^{s} is the mean energy collected by ions at the surface of graphene sheet,

ε is the emissivity of the material of the graphene sheet, and

σ is the Stefan–Boltzmann constant.

Eq. (4.13) illustrates the effect of RF power on the mass of the graphene sheet. The first two terms in Eq. (4.13) represents the rate of energy transferred to the graphene sheet due to sticking accretion and elastic collision by constituent species of complex plasma. The third term accounts the ionization of neutral species 1 and 2 resulting in the collection of ions on the surface of graphene sheet, and the fourth term is due to sticking accretion of ions 1 and 2 on the graphene surface. The last term is the rate of energy dissipation of the graphene through radiation and conduction to the host gas.

4.9 Field enhancement factor

Following Watcharotone et al. [46] and Miller et al., [47] the expression for the field enhancement factor of graphene can be written as

$$\beta \approx \frac{h}{t} \qquad \text{...(4.14)}$$

where,

h is the height of the graphene sheet, and

t is the thickness of the graphene sheet.

Chapter 5: Results and Discussion

Numerical calculations have been carried out to study the dependence of the dimensions (i.e., thickness and height) of the graphene sheet on the plasma composition (i.e., different fractional light ion concentrations), which subsequently influence its field emission properties.

We have solved Eqs. (3.1)–(3.13) simultaneously at the appropriate boundary conditions, viz., at $\tau = 0$;

Table 1

electron number density n_{eo}	$=10^{12}$ cm^{-3}
ion number density, n_{iha}	$= (1\text{-}a_l)n_{eo}$
ion number density, n_{ilb}	$= (a_l)n_{eo}$
neutral atom density $n_{hao} = n_{lbo}$	$= 10^{14}cm^{-3}$
electron temperature T_{e0}	= 1.7 eV
ion temperature T_{i0}	= 2200 K
neutral temperature T_{n0}	= 2000 K
mass of heavy ion 'a' m_{ha}	= 26 a.m.u for acetylene ($C_2H_2^{+}$)
mass of light ion 'b' m_{lb}	= 1amu for (H^{+})
density of catalyst Cu ρ_{ct}	$= 8.96$ g/cm^3
coefficient of recombination of electrons and ions $\alpha_{10} \approx \alpha_{20}$	$= 1.12 \times 10^{-7}$ cm^3/s
κ	= -1.2
substrate temperature T_s	= 600 ^oC

Other parameters used in the calculations are

Table 2

thermal energy barrier on the catalyst surface δE_i	= 1.87 eV
energy barrier for diffusion of carbon monomers E_{sdC}	= 0.1 eV
energy barrier for carbon clusters E_{sdCl}	= 0.82 eV
energy due to dehydrogenation of C_2H_2 δE_{sdh}	= 1.7 eV
sticking coefficient of electron γ_e	=1
sticking coefficient of ion γ_{ij}	=1

With the help of MATHEMATICA software and using all the above values, we solve all the differential Eqs. (4.1)–(4.13) simultaneously to study the dependence of height and thickness of graphene sheet on plasma parameter(i.e., different fractional light ion concentrations).

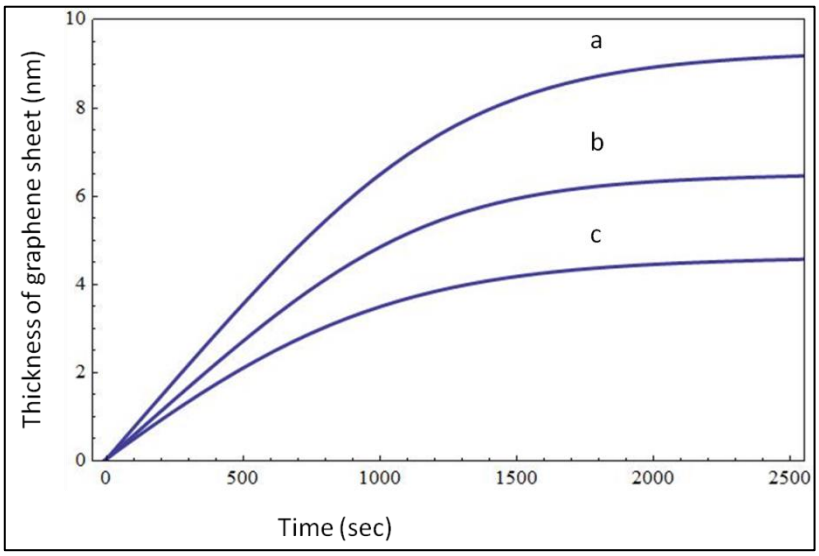

Figure 5.1. Variation of the thickness for graphene sheet for different fractional concentrations of light positive charged ions (i.e. a, b, c corresponds to a_l = 0.3,0.6 & 0.9, respectively).

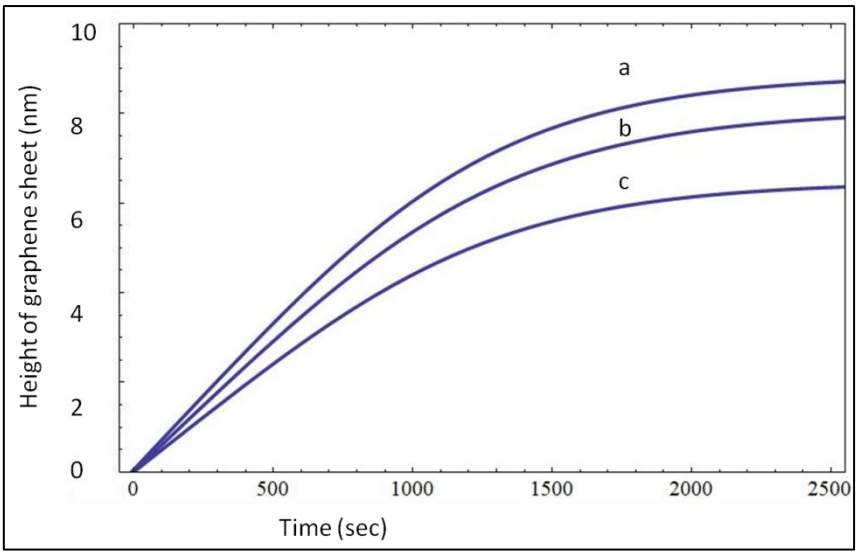

Figure 5.2. Variation of the height for graphene sheet for different fractional concentrations of light positive charged ions. (i.e a, b, c corresponds to a_l = 0.3,0.6 & 0.9, respectively)

From Fig. 5.1 and Fig. 5.2, it can be seen that the thickness and height of graphene sheet first increases with time and then attains a saturation value. It also shows the

decrease of thickness 't' and height 'h' with fractional concentrations of light positively charged ions, a_l . The growth of graphene on catalyst-substrate surface proceeds by two processes, namely, surface deposition by carbon species and etching of the graphene sheet. On increasing light positively charged ions, the etching of the graphene sheet increases, leading to decrease of the thickness of the graphene sheet. Moreover, on increasing a_l, the number of carbon atoms responsible for growth of graphene also decreases due to formation of volatile by products such as CH, thereby, the height and thickness of the graphene sheet decreases on increasing a_l.

From the above result, we can tune the plasma composition (i.e., a_l) to vary the graphene sheet's height and thickness. As per the above results, the change in height with a_l is not much pronounced in comparison to change in thickness.

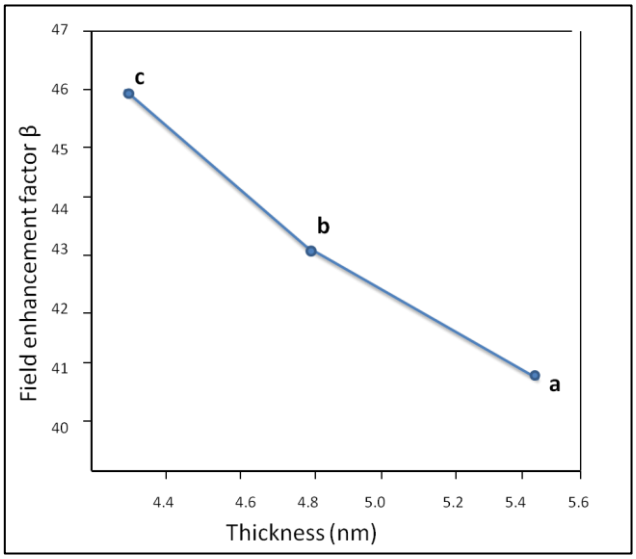

Figure. 5.3. Variation of field enhancement factor b with the thickness of graphene sheet corresponding to different fractional concentration values of light ion a_l (where a, b and c corresponds to different values of different fractional concentration values of light ion, i.e., a(0.3), b (0.6), and c(0.9).

so further looking at the effect of plasma composition on the field emission factor β $\approx \frac{h}{t}$, where h is the height and t is the thickness of graphene sheet) . It is found that the field enhancement factor increases with the increase in the plasma composition (fractional concentrations of light positively charged ions) as shown in figure 5.3

Chapter 6: Conclusion

In the present analysis, a theoretical model comprising charging rate equation of the graphene sheet; kinetic equations of neutral atoms, ions & electrons; kinetic equations for the growth of graphene nuclei; growth rate equation for the graphene sheet has been developed. We have varied the concentrations of participating light positively charged ions and studied its effect on graphene sheet dimensions. From calculations we have observed the dependence of the graphene sheet dimensions on the various compositions of ions in plasma i.e., by varying n_{ihA0} and n_{ilB0}. Different plasma compositions signify the different concentrations of participating ions.

It is found that by varying fractional light ion concentration, the thickness and height of graphene sheet decreases and consequently the field emission factor β ($\approx \frac{h}{t}$, where h is the height and t is the thickness of graphene sheet) increases.

.

References

1. Novoselov, Kostya S., Andre K. Geim, S. V. Morozov, D. Jiang, Y_ Zhang, SV and Dubonos, I. V. Grigorieva, and A. A. Firsov. (2004), science, Vol. 306, p. 666.
2. C. S. Lee, B. Khang, and A. L. Barabási, (2001) Appl. Phys. Lett. 78, 984.
3. Schafheutl, C. (1840) Philos. Mag., 16, 570.
4. Brodie, B.C. (1859) Philos. Trans. R. Soc. London, 149, 249.
5. Staudenmaier, L. (1898) Ber. Dtsch. Chem. Ges., 31, 1481.
6. Hummers, W.S. and Offeman, R.E. (1958) J. Am. Chem. Soc., 80, 1339.
7. Bourlinos, A.B., Gournis, D., Petridis, D., Szabo, T., Szeri, A., and Dekany, I. (2003) Langmuir, 19, 6050.
8. Allen, M.J., Tung, V.C., and Kaner, R.B. (2010) Chem. Rev., 110, 132.
9. Prezhdo, O.V. (2011) Surf. Sci., 605, 1607.
10. Novoselov, K.S., Geim, A.K., Morozov, S.V., Jiang, D., Zhang, Y., Dubonos, S.V., Grigorieva, I.V., and Firsov, A.A. (2004) Science, 306, 666.
11. Meyer, J.C., Geim, A.K., Katsnelson, M.I., Novoselov, K.S., Booth, T.J., and Roth, S. (2007) Nature, 446, 60–63.
12. Castro, N., Guinea, F., Peres, N.M.R., Novoselov, K.S., and Geim, A.K. (2009) Rev. Mod. Phys., 81, 109.
13. Frank, I.W., Tanenbaum, D.M., van der Zande, A.M., and McEuen, P.L.J. (2007) Vac. Sci. Technol., 25, 2558–2561.
14. Edwards, R.S. and Coleman, K.S., 2013. Nanoscale, 5(1), pp.38-51.
15. Su, C.Y., Lu, A.Y., Xu, Y., Chen, F.R., Khlobystov, A.N. and Li, L.J., 2011 ACS nano, 5(3), pp.2332-2339.
16. Wang, G., Shen, X., Wang, B., Yao, J. and Park, J., 2009., 47(5), pp.1359-1364.
17. Huang, H., Xia, Y., Tao, X., Du, J., Fang, J., Gan, Y. and Zhang, W., 2012 Journal of Materials Chemistry, 22(21), pp.10452-10456.
18. Emtsev, K.V., Bostwick, A., Horn, K., Jobst, J., Kellogg, G.L., Ley, L., McChesney, J.L., Ohta, T., Reshanov, S.A., Röhrl, J. and Rotenberg, E., 2009.. Nature materials, 8(3), pp.203-207.
19. Riedl, C., Coletti, C., Iwasaki, T., Zakharov, A.A. and Starke, U., 2009. Physical review letters, 103(24), p.246804.
20. Woodworth, A.A. and Stinespring, C.D., 2010. Carbon, 48(7), pp.1999-2003

21. www.nobelprize.org/nobel_prizes/physics/laureates/2010/advanced-physicsprize2010.pdf
22. Incorporation of Plasma into CVD graphene growth Jacob Arwe, Xuan Gao, Department of Physics, Case Western Reserve University
23. A. Rhallabi, Y. Catherine, *IEEE Trans. Plasma Sci.* 1991, 19, 270.
24. N. Mutsukura, S. Inoue, Y. Machi, *J. Appl. Phys.* 1992, 72, 43.
25. J. L. Pack, R. E. Voshall, A. V. Phelps, L. E. Kline, *J. Appl. Phys.* 1992, 71, 5363.
26. D. Herrebout, A. Bogaerts, M. Yan, R. Gijbels, W. Goedheer, E. Dekempeneer, *J. Appl. Phys.* 2001, 90, 570.
27. D. Herrebout, A. Bogaerts, M. Yan, R. Gijbels, W. Goedheer, A. Vanhulsel, *J. Appl. Phys.* 2002, 92, 2290.
28. I. B. Denysenko, S. Xu, J. D. Long, P. P. Rutkevych, N. A. Azarenkov, K. Ostrikov, *J. Appl. Phys.* 2004, 95, 2713.
29. K. Ostrikov, H. J. Yoon, A. E. Rider, S. V. Vladimirov, *Plasma Processes Polym.* 2007, 4, 27.
30. D. Hash, D. Bose, T. R. Govindan, M. Meyyappan, *J. Appl. Phys.* 2003, 93, 6284.
31. T. Terasawa, K. Saiki, *Carbon* 2012, 50, 869.
32. L. C. Zhang, Z. W. Shi, Y. Wang, R. Yang, D. X. Shi, G. Y. Zhang, *Nano Res.* 2011, 4, 315.
33. W. Yang, C. L. He, L. C. Zhang, Y. Wang, Z. W. Shi, M. Cheng, G. B. Xie, D. M. Wang, R. Yang, D. X. Shi, G. Y. Zhang, *Small*
34. H. Mehdipour, K. Ostrikov, *ACS Nano* 2012, 6, 10276.
35. D. H. Liu, W. Yang, L. C. Zhang, J. Zhang, J. L. Meng, R. Yang, G. Y. Zhang, D. X. Shi, *Carbon* 2014, 72, 387.
36. Y. H. Wu, P. W. Qiao, T. C. Chong, Z. X. Shen, *Adv. Mater.* 2002, 14, 64.
37. Y. Chai, Z. Xiao, P. C. H. Chan, *Appl. Phys. Lett.* 2009, 94, 043116.
38. L. L. Jiang, T. Z. Yang, F. Liu, J. Dong, Z. H. Yao, C. M. Shen, S. Z. Deng, N. S. Xu, Y. Q. Liu, H. J. Gao, *Adv. Mater.* 2013, 25, 250.
39. Li M., Liu D., Wei D., Song X., Wei D., Wee A. T. S. (2016). Adv. Sci., 3: 1600003. doi: 10.1002/advs.201600003
40. A. Tewari and S. C. Sharma, Phys. Plasmas 21, 063512 (2014).
41. Suresh C. Sharma and Neha Gupta, Phys. Plasmas 22, 123517 (2015).

42. H. Mehdipour and K. Ostrikov, ACS Nano 6, 10276 (2012).
43. I. Denysenko and K. Ostrikov, J. Phys. D: Appl. Phys. 42, 015208 (2009).
44. M. Zhu, J. Wang, B. C. Holloway, R. A. Outlaw, X. Zhao, K. Hou, V. Shutthanandan, and D. M. Manos, Carbon 45, 2229 (2007).
45. M. S. Sodha, S. Misra, S. K. Misra, and S. Srivastava, J. Appl. Phys. 107, 103307 (2010).
46. S. Watcharotone, R. S. Ruoff, and F. H. Read, Phys. Proc. 1, 71 (2008).
47. R. Miller, Y. Y. Lau, and J. H. Booske, Appl. Phys. Lett. 91, 074105 (2007).
48. A. Tewari , R. Walia , and S.C. Sharma, Phys. Plasmas 19 013502 (2012).